Hindawi
Journal of Nanomaterials
Volume 2018, Article ID 9456971, 8 pages
https://doi.org/10.1155/2018/9456971

Research Article

Micromorphology and Mechanical and Dielectric Properties of Bismaleimide Composite Modified by Multiwalled Carbon Nanotubes and Polyethersulfone

Yufei Chen,[1,2] **Chengbao Geng**,[2] **Yang Han**,[2] **Mingzhuo Chai**,[2] **Hongyuan Guo**,[2] **Chunyan Yue**,[2] **and Yingyi Ma**[2]

[1]*Key Laboratory of Engineering Dielectrics and Its Application, Ministry of Education, Harbin University of Science and Technology, Harbin 150080, China*
[2]*The College of Materials Science and Engineering, Harbin University of Science and Technology, Harbin 150040, China*

Correspondence should be addressed to Yufei Chen; chenyufei@hrbust.edu.cn

Received 19 June 2018; Revised 19 September 2018; Accepted 4 October 2018; Published 19 November 2018

Guest Editor: Bathula Babu

Multiwalled carbon nanotubes (MWCNTs) were modified by oxidizing agent to obtain O-MWCNTs, and the surface of it was coated with active group. 4,4′-Diaminodiphenylmethane bismaleimide (MBMI) was used as matrix, 3,3′-diallyl bisphenol A (BBA) and bisphenol-A diallyl ether (BBE) were used as reactive diluent, polyethersulfone (PES) as toughening agent, and O-MWCNTs as modifier; OMWCNT/PES-MBAE composite was prepared through in situ sol-gel method. The effect of PES and OMWCNTs on the mechanical and dielectric properties of composite was analyzed, and the microstructure was examined by transmission electron microscope (TEM) and scanning electron microscope (SEM). The mechanism of composite toughened by PES and OMWCNTs was observed and analyzed. The results showed that Diels-Alder reaction between MBMI and allyl compounds occurred completely and unsaturated double bond disappeared. O-MWCNTs and PES resin dispersed smoothly in polymer matrix and were used as reinforcement, and PES resin and O-MWCNTs could synergistically improve the properties of the composite and exhibited a typical ductile fracture. The impact and bending strengths were 16.09 kJ/m^2 and 153.57 MPa, which were 74.32% and 53.08% higher than those of the MBAE matrix, respectively, and the dielectric constant and the dielectric loss were 3.76 (100 Hz) and 2.79×10^{-3} (100 Hz), when the content of PES was 2 wt% and O-MWCNTs was 0.02 wt%. The outstanding properties of the material made it play an important role in high-performance insulating material applications.

1. Introduction

Bismaleimide (BMI) is a kind of outstanding polymer matrix; due to its excellent processability, heat resistance, radiation resistance, and good insulation properties, it is widely used in aerospace field and electrical insulating materials, such as aircraft floor, isolation wall, exhaust system and piping, and other components. In addition, combined with carbon fiber, it can also be used for aircraft bearing or nonbearing structural parts, wing skin, tail, aircraft fuselage, and skeleton. However, unmodified BMI cannot meet the requirements of processing and using; due to its high brittleness and bad shock resistance, the toughening modification of BMI resin is a hot topic all the time [1, 2]. Li et al. reported that PDMS-AN/BDM composite has a flexural strength of 80.74 MPa, a flexural modulus of 3294.72 MPa, and an impact strength of 8.06 kJ/m^2 [3]. Ji and coworkers reported that a reactive hyperbranched polysiloxane (HPSiE) terminated by epoxy groups was designed and synthesized to develop a novel high-performance modified bismaleimide-triazine resin, resulting in an impact strength of 16.5 kJ/m^2 [4]. Yan et al. prepared novel bismaleimide nanocomposites with Si_3N_4 nanoparticles; the highest impact strength and flexural strength were 15 kJ/m^2 and 85 MPa, respectively [5]. These studies have improved the properties of bismaleimide resin to some extent. Polyethersulfone (PES) is one of the most widely used special engineering plastics; it has excellent heat resistance, physical and mechanical properties,

insulation properties, and so on; and it can keep the stability of performance at high temperatures and can be usually used as a toughening agent to improve the toughness of BMI resin [6, 7].

In recent years, carbon nanotechnology has been the focus of research and is widely used in many fields, due to their excellent physical and chemical properties, and the development of carbon nanomaterials has promoted the progress in materials, medicine, chemical engineering, artificial intelligence, and other fields. Multiwalled carbon nanotube (MWCNT) is a new type of high-strength carbon material, which has unusual mechanical, electrical, and chemical properties, and it is usually used as effective reinforcement of the composite; exhibits good strength, elasticity, fatigue resistance, and isotropy; and greatly improves the performances of the composite [8–10]. Unmodified MWCNTs are prone to reunite in the polymer matrix, so the modification of MWCNTs is very important [11, 12]. In this paper, multiwalled carbon nanotubes (MWCNTs) were modified by concentrated sulfuric acid to obtain O-MWCNTs. 4,4′-Diaminodiphenylmethane bismaleimide (MBMI) was used as matrix, 3,3′-diallyl bisphenol A (BBA) and bisphenol-A diallyl ether (BBE) were used as reactive diluent to synthesize polymer matrix (MBAE), polyethersulfone (PES) was used as toughening agent, and OMWCNTs was used as modifier; O-MWCNT/PES-MBAE composite was prepared through in situ sol-gel method. And then, the morphology of MWCNTs and O-MWCNT/PES-MBAE composite was observed by TEM and SEM, respectively. Furthermore, the mechanical and dielectric properties of the composite were discussed; PES and O-MWCNTs have a good compatibility with the resin matrix and can synergistically toughen the resin matrix. The study can provide a valuable reference for further application of BMI resin in the engineering field.

2. Experimental

2.1. Materials. Multiwalled carbon nanotubes (MWCNTs) were purchased from Guangzhou Hongwu Material Technology Co. Ltd. (CHN); the diameter is 40–60 nm, and the length is 5–15 μm. 4,4′-Diaminodiphenylmethane bismaleimide (MBMI), a yellow powder with a melting point of 155°C, has a density of 1.43 g/cm^3. 3,3′-diallyl bisphenol A (BBA) and bisphenol-A diallyl ether (BBE) were all purchased from Laizhou Laiyu Chemical Co. Ltd. (CHN); BBA is a light yellow liquid with a density of 1.08 g/cm^3, and BBE is a colorless liquid with a density of 1.03 g/cm^3. Polyethersulfone (PES) was from Changchun Jida Special Plastic Engineering Co. Ltd. (CHN); the molecular weight is 30,000; the intrinsic viscosity is 0.32; and the continuous use temperature is about 180–200°C. Concentrated sulfuric acid (H_2SO_4) and concentrated nitric acid (HNO_3), chemically pure, were purchased from Shanghai Chemical Reagent Factory (CHN).

2.2. Modification of MWCNTs. Four grams of pristine MWCNTs and 100 ml solution of sulfuric acid and nitric acid mixture with a volume ratio of 3 : 1 were added into a round bottom flask, MWCNT/acid mixture flask was sonicated for 20 min in an ultrasonic bath at 70°C in order to prevent agglomeration of MWCNTs, then the cooled mixture was diluted with deionized water and washed subsequently until the pH value was about 7, and finally O-MWCNTs were obtained by the removal of residual solvent under vacuum.

Table 1: The type and component of the composite.

Number of samples	Component	PES content (wt%)	O-MWCNT content (wt%)
A	MBAE	0	0
B0	PES-MBAE	2	0
B1	MWCNTs/PES-MBAE	2	0.01
B2	MWCNTs/PES-MBAE	2	0.02
B3	MWCNTs/PES-MBAE	2	0.03
B4	MWCNTs/PES-MBAE	2	0.04

2.3. Preparation of O-MWCNT/PES-MBAE Composite. The mixed solution of BBA and BBE was gotten in a mass ratio of 3 : 2, transferred to a three-necked flask, and stirred for 15 min at 70°C in an ultrasonic cleaner; O-MWCNTs were added into the solution and stirred for 2 h. Then, PES resin was added into the mixture at 170°C and finally stirred until they were dispersed evenly. MBMI was dispersed in the above solution at 130°C and obtained a uniform mixture, and the mixture was removed to a preheated mold and was in a vacuum oven. The curing process was carried out at five steps; 130°C/1 h, +150°C/1 h, +180°C/1 h, +200°C/1 h, and +230°C/1 h. The samples were numbered as in Table 1.

2.4. Measurements. The surface morphology of O-MWCNTs and composites were characterized by transmission electron microscope (TEM, JEM-2100 UHR, JEOL Ltd., Tokyo, Japan) and by scanning electron microscope (SEM, JAPA). Samples were deposited on a sample holder with adhesive carbon foil and were sputtered with gold.

The FT-IR spectra, which were used to study the chemical structure of the materials, were performed with an Equinox-55 Fourier-transform spectrometer (GER), in the 400–4000 cm^{-1} range. And it could be seen that there existed the characteristic absorption peaks of the materials.

The impact strength of specimens was tested by Charpy impact machine tester (Jinan Huaxing Laboratory Equipment Co. Ltd.), according to the standard of GB/T 2567-2008, and the specimens needed no bubbles, cracks, scars, and other defects. For each sample, five measurements were made at least and the average value was taken; the test was carried out at room temperature.

The bending strength of samples was tested by CSS-44300 electronic testing machine (Shanghai Technical Instrument Co. Ltd., CHN) according to the standard of GB/T 2567-2008. Standard of bending strength experiments was performed at room temperature, with a speed of 2 mm/min. For each sample, five measurements were made at least and the average value was taken.

Dielectric constant (ε) and dielectric loss (tanδ) of the composite material were measured with Agilent-4292A

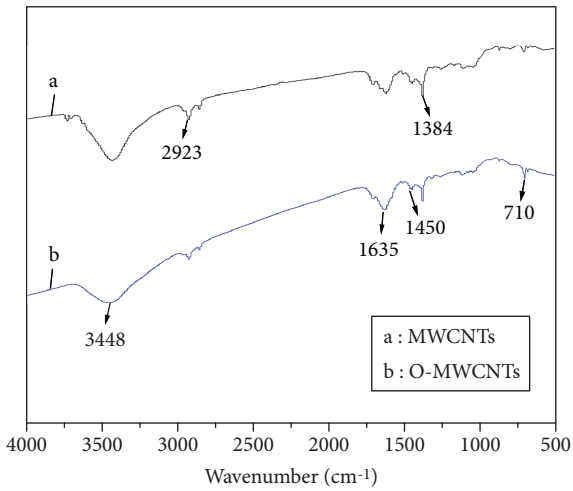

Figure 1: FT-IR spectra of MWCNTs.

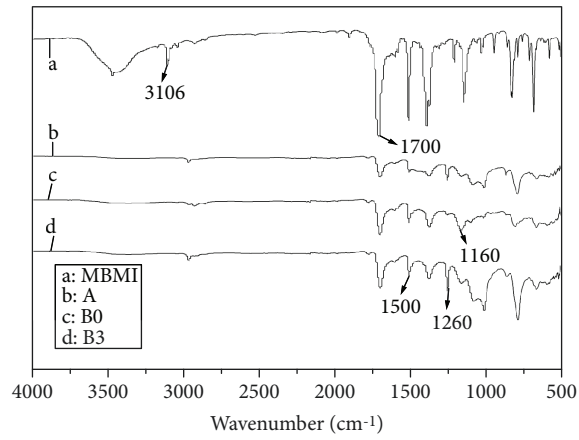

Figure 2: FT-IR spectra of the composite.

precise impedance analyzer (Japan) in the frequency range of 100 Hz–100 kHz at room temperature according to GB/T 1409-2006.

3. Results and Discussions

3.1. FT-IR Spectral Analysis. FT-IR spectra of MWCNTs and O-MWCNTs were presented in Figure 1. The peak at 1450 cm^{-1} was the stretching vibration of carbon skeleton, and the peaks at 2923 cm^{-1} and 1384 cm^{-1} were the asymmetrical stretching vibration of -CH_2- and the symmetrical bending vibration of -CH_3-, respectively. The broad peak at 3448 cm^{-1} was the stretching vibration of intermolecular associative -OH in curve b, and the peaks at 1635 cm^{-1} and 710 cm^{-1} were the stretching vibration of -C=O and S-O, respectively. It revealed that a certain amount of carboxyl groups has been deposited in the surface of O-MWCNTs [13].

FT-IR spectra of materials were exhibited in Figure 2. The curves a, b, c, and d represented MBMI resin, MBAE matrix, PES-MBAE, and O-MWCNT/PES-MBAE composite, respectively.

In curve a, the peak at 3106 cm^{-1} was caused by the stretching vibration of C=C in MBMI; however, this characteristic peak vanished in curves b, c, and d. The emergence of this phenomenon corroborated that the Diels-Alder reaction between MBMI and allyl compounds has taken place [14]. In curves a, b, c, and d, the peaks at 1700 cm^{-1} and 1500 cm^{-1} were the stretching vibration of C=O and the stretching vibration of C=C in the benzene ring skeleton, respectively. The peak at 1160 cm^{-1} was the stretching vibration of O=S=O in curves c and d. The peak of curve d at 1260 cm^{-1} was caused by the stretching vibration of C-O and indicated that the O-MWCNTs have been doped to the composite [15]. The results of FT-IR spectra suggested that O-MWCNT/PES-MBAE composite has been prepared successfully.

3.2. Analysis of TEM Patterns. The micromorphology of MWCNTs and O-MWCNTs was investigated by TEM in Figure 3, so as to observe the effect of modification and verify the above results.

Figure 3 displayed the TEM images of MWCNTs and O-MWCNTs; Figure 3(a) shows the MWCNTs; Figures 3(b) and 3(c) show the O-MWCNTs, the magnification was 4×10^4 times and 1×10^4 times, respectively; and Figure 3(d) image shows the energy spectrum of the selected region. In Figure 3(a), it would be seen that MWCNTs were scrolls and intertwined and exhibited nanowire-like morphology and a smooth surface with nothing adhering to them, as it was a stable structure of C=C bond and had no active group. The oxidation of MWCNTs by strong acid treatment significantly alters the surface roughness of nanotubes. Figures 3(b) and 3(c) showed that the reunion of O-MWCNTs weakened, the ratio of length and diameter did not change, and its walls became rough and had many active cross-linking points; this was because there were more defects on its surface; hydroxy groups and carboxyl groups appeared at the defects to form active cross-linking points [16]. The energy spectrum was used to analyze element component in order to explore the function of modification. Figure 3(d) shows the energy-spectra of O-MWCNTs; the surface of the marked area was broken and formed hollow. In the selected area, C element was dominant; the weight ratio of N, O, and S elements was lower, 1.7 wt%, 2.7 wt%, and 0.3 wt%; the nitrified degree and sulfonated degree were about 7.65% and 0.92%, respectively. It is indicated that the surface of O-MWCNTs had active groups of $-SO_3H$ and $-NO_2$; these polar groups could make the compatibility better between MWCNTs and resin matrix and do not destroy the structure of MWCNTs [17, 18].

3.3. Analysis of SEM Patterns. The microscale cross-section morphology of the material could be studied by the SEM, and the pictures of the composite were shown in Figure 4. Figures 4(a) and 4(b) show the morphology of sample A, Figures 4(c) and 4(d) show sample B0, and Figures 4(e) and (f) show sample B2. Figures 4(a) and 4(b) showed that the fracture surface of sample A had no obvious microcracks and was a typical morphology of brittle fracture; the reason

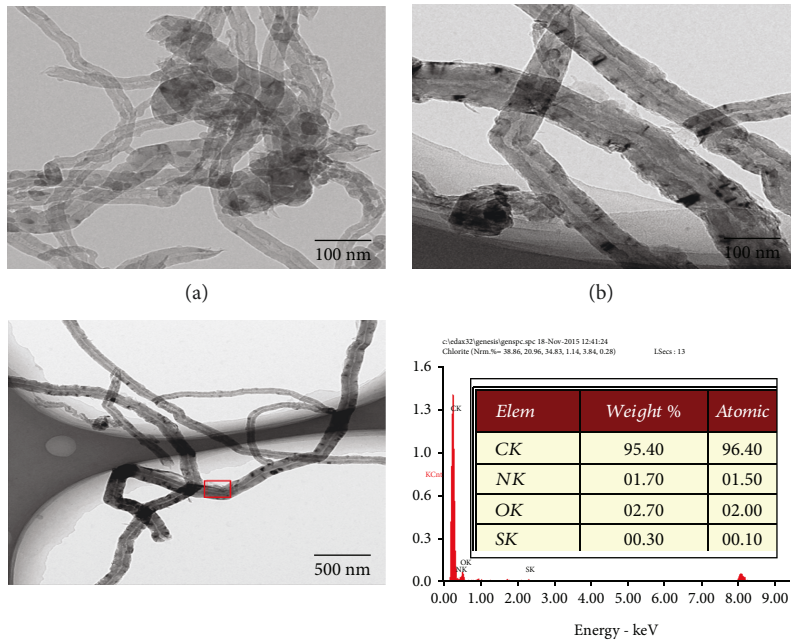

Figure 3: TEM patterns and energy spectrum of MWCNTs.

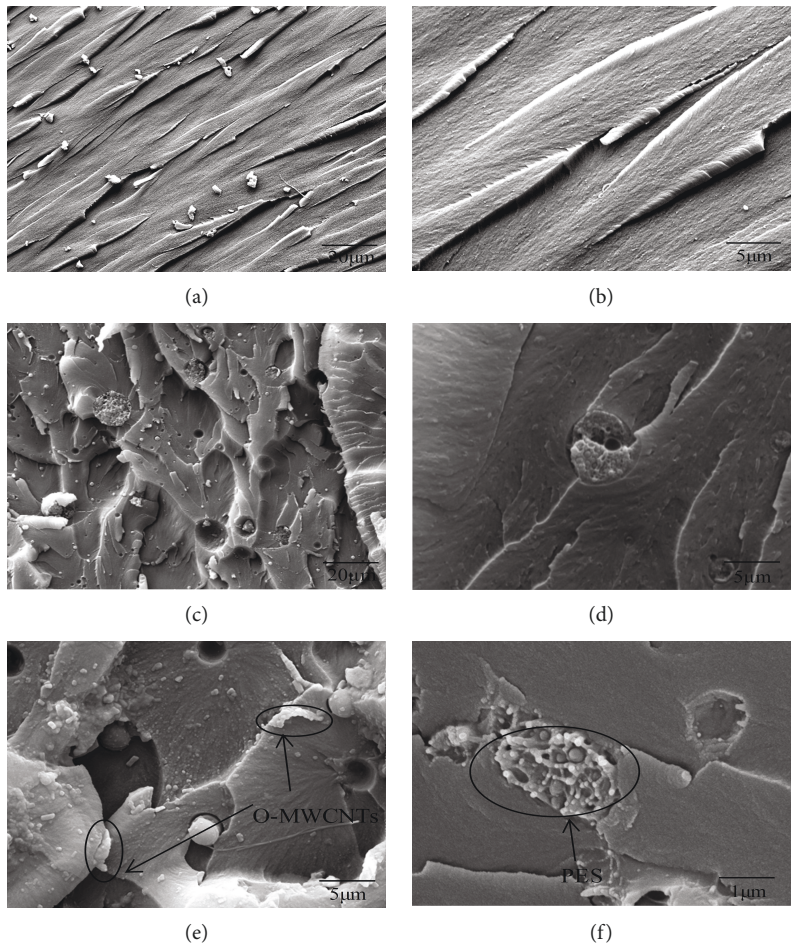

Figure 4: SEM photographs of the composite: (a) A ×1000, (b) A ×5000, (c) B0 ×1000, (d) B0 ×5000, (e) B2 ×5000, and (f) B2 ×20,000.

was that the chemical structure of MBMI was symmetric and the crystallinity could lead the material to become brittle. There existed many "honeycombs" in Figures 4(c) and 4(d); the size of its scale was about 5 μm and it was a PES resin [19]. It could be seen that the PES particles were inlaid in the matrix and presented as a two-phase structure in the composite. The cross-section surface of PES-MABE had obvious microcracks, and the fracture was ductile; the main reason was that the PES phase evenly dispersed in continuous MABE phase and the interaction between two phases was strong. The material would crack along the direction of the force when the composite suffered external force; a great number of microcracks formed as the interface function between two phases combined well and played a role of toughening effects [20, 21]. The formation of microcracks and shear zone could absorb a quantity of energy and cause a ductile fracture.

SEM pictures of sample B2 were displayed in Figures 4(e) and 4(f); it could be distinctly seen that PES resin and O-MWCNTs were uniformly dispersed in the matrix; due to the presence of active groups on the surface of O-MWCNTs, these groups could cross-bond with polar groups of the matrix and PES resin [22], and O-MWCNTs and PES resin had synergistical toughening effects. The mutual entanglement between MWCNTs was weakened, and the interaction with the matrix was enhanced, thereby, to improve the dispersion of the PES resin in the matrix. In addition, there are mutual infiltration and interpenetration between PES resin and the matrix. When the PES phase encountered the external force during the fracture process, the cracks were passivated, and the direction of the cracks had changed. This effect was beneficial to improve the performance of the composite; meanwhile, there are polar groups on the surface of O-MWCNTs and PES resin, and they would form a synergistic effect [23–25]. When the composite suffered external force, this synergistic effect would hinder the development of microcracks and absorb a quantity of energy to enhance the interaction between the phase interfaces. Therefore, the composite of O-MWCNTs/PES-MBAE exhibited a typical ductile fracture.

3.4. Mechanical Properties of Composite. Impact strength and bending strength were two important indicators of mechanical properties; their results were shown in Table 2. Their tendency was increased first and then decreased, and the properties of sample B2 was the best; impact strength and bending strength were 16.09 kJ/m^2 and 153.57 MPa, which were higher by 74.32% and 53.08% than that of sample A, respectively. This indicated that PES resin and O-MWCNTs had a great influence on the mechanical properties of composites to some extent. The main reasons were that the PES resin could disperse in the polymer matrix and present a two-phase structure according to the SEM results, and the toughening theory of PES accorded with outside toughening mechanism; the interfaces formed due to the interaction among continuous phase (MBAE), PES, and O-MWCNTs. Additionally, O-MWCNTs had good compatibility with the system and could be evenly dispersed in the matrix resin and simultaneously formed a synergistic effect with the PES resin. The interaction among three components was enhanced, which effectively prevented the development of cracks and absorbed more energy when the material was broken. In the bending process of material, the external force firstly caused stress yield and a large number of silver streak and microcracks appeared inside the material and finally formed a macroscopic fracture [26]. O-MWCNTs could effectively suppress the development of microcracks in the yielding process of material and could block the microcracks and change its developing direction to make the microcracks develop irregularly; when the silver streak or microcracks appeared, it was beneficial to improve the mechanical properties of the composite.

Table 2: Impact strength and bending strength of the composite.

Type	Impact strength (kJ/m^2)	Increasing rate (%)	Bending strength (MPa)	Increasing rate (%)
A	9.23	0	100.32	0
B0	10.36	12.24	117.36	16.99
B1	13.37	44.85	124.09	23.69
B2	16.09	74.32	153.57	53.08
B3	14.41	56.12	128.64	28.22
B4	12.73	37.92	121.04	20.65

3.5. Dielectric Properties of Composite. Dielectric constant and dielectric loss were two important characteristic indicators of the dielectric materials. The internal factors of influencing dielectric constant were the condition of dielectric polarization and polarization divided into electronic polarization, atomic polarization, orientation polarization, and interfacial polarization according to different molecular polarization mechanisms. The dielectric constant of polar molecule depended on the orientation polarization and increased with the increasing of polarization extent. Figure 5 displayed the dielectric constant curves of the composite. The permittivity of the composite decreased gradually with the increasing frequency (from 10^2 to 10^6 Hz); nevertheless, the rate of descent was accelerated when the frequency was over 10^4 Hz. At low frequency, the dielectric constant varied slowly, the period of the variation was much longer than the relaxation time, and the polarization was completely comparable to the electric field. At high frequency, the electric field varied rapidly, the period was very short and almost much shorter than the relaxation time, the relaxation polarization could not keep up with the variation of the electric field, and the instantaneous polarization occurred; it led to the decrease of the permittivity [27].

The permittivity of sample B0 was higher than that of sample A. On the one hand, the PES resin contained polar groups and the density of the polar groups increased. On the other hand, the PES resin formed an interface with the matrix resin, which could absorb a large amount of charge and initiate interface polarization; therefore, the permittivity of materials increased slightly.

The dielectric constant of O-MWCNT/PES-MBAE composite was lower than that of sample B0, and sample A was

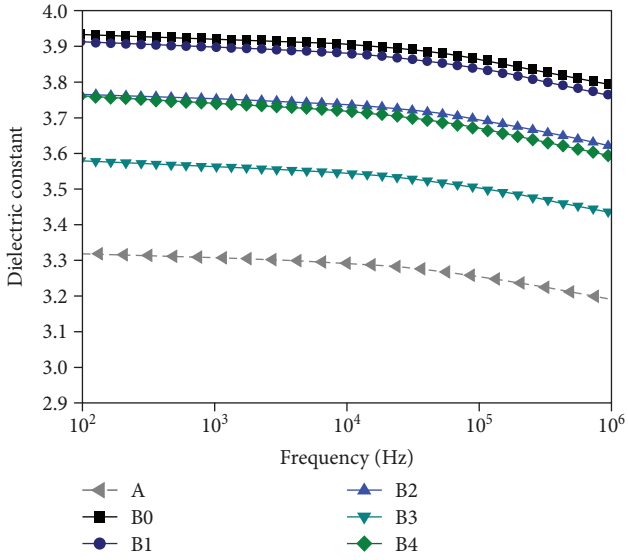

Figure 5: Dielectric constant of the composite.

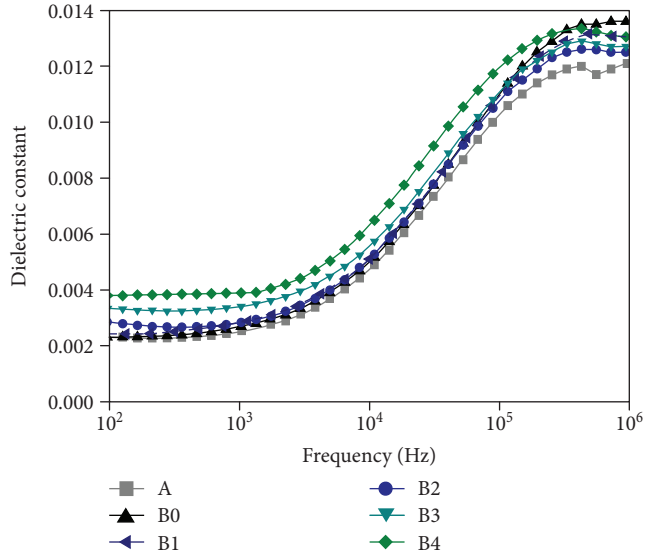

Figure 6: Dielectric loss of the composite.

the lowest at the same frequency. Commonly, the addition of O-MWCNTs would increase the conductivity and decrease the dielectric constant. However, with the increase of O-MWCNT doping content, the binding density increased, the chain segment motion of polymer was hindered by the binding entanglement effect, and the orientation polarization of the dipole in the system was restrained. Due to a little doping amount of O-MWCNTs, the effect of binding entanglement played a dominant role, resulting in the decrease of dielectric constant [28]. When the content of O-MWCNTs was 0.04 wt%, the interface interaction between the O-MWCNTs and the resin matrix increased, the binding effect of carriers in the interface overlap region was weakened, the interfacial polarization was enhanced, and the migration of carriers became easy, so the permittivity of materials increased.

Figure 6 showed the dielectric loss curves of the composite; the frequency was from 10^2 Hz to 10^6 Hz. The dielectric loss of the composite was 0.002 to 0.004 with the slight fluctuation at low frequency (10^2–10^3 Hz), but the dielectric loss increased rapidly at 10^3 Hz–10^5 Hz. The reasons were probably that the polarization could completely keep up with the change of the electric field at low frequency, and the absorbed energy could be returned to the electric field in time, so the dielectric loss was smaller. At high frequency, the orientation polarization needed to overcome the internal resistance of the material, while the dipole steering lagged behind the variation of the electric field and the relaxation phenomenon was obvious [29]. When the frequency was adequately high, the orientation polarization needed a long time in the relaxation process, so the variation of the dielectric loss was small at this time.

The dielectric loss of sample A was the lowest, sample B0 was the second, and the dielectric loss of O-MWCNTs/PES-MBAE composite was slightly higher than that of the others at the same frequency. This phenomenon could be explained as follows: the cross-linking density declined because the PES resin presented as a two-phase structure in the matrix, and the friction resistance increased due to the interaction between PES and matrix. A large number of interfaces were formed, which caused the dipole's steering to be suppressed, and more energy was required to overcome the friction resistance. At the same time, the PES resin carried with polar groups and the relaxation polarization ability increased, so the dielectric loss of sample B0 increased [30, 31]. Additionally, O-MWCNTs may carry with carriers to material and generate a conductive current when the electric field was applied to the composite. Therefore, the dielectric loss increased with the addition of O-MWCNTs. Because the content of O-MWCNTs was very low, the dielectric loss was still ideal, and the insulation performance of the composite material could meet the applied requirement.

4. Conclusions

O-MWCNTs have good compatibility with the polymer matrix, the Diels-Alder reaction between MBMI and allyl compounds has taken place, and the O-MWCNT/PES-MBAE composite has been prepared. PES resin evenly disperses in a "honeycomb" two-phase structure in the MBAE matrix. PES resin and O-MWCNTs can synergistically toughen the composite, and O-MWCNTs/PES-MBAE composite exhibits a typical ductile fracture. The comprehensive performance of O-MWCNT/PES-MBAE composite is the best when the content of PES resin is 2 wt% and O-MWCNTs is 0.02 wt%; the impact and bending strengths are 16.09 kJ/m^2 and 153.57 MPa, which are 74.32% and 53.08% higher than those of MBAE matrix, respectively. The permittivity and the dielectric loss of O-MWCNT/PES-MBAE composite are 3.76 (100 Hz) and 2.79×10^{-3} (100 Hz). O-MWCNTs could greatly improve the mechanical properties of the composite material, and its dielectric properties have decreased slightly; its performance could meet the requirement of insulating material.

Data Availability

All data included in this study are available upon request by contact with the corresponding author.

Conflicts of Interest

The authors declare that there is no conflict of interests regarding the publication of this paper.

Acknowledgments

The authors would like to express their appreciation to the project support by the Natural Science Foundation of China (21604019) and the Harbin Technology Bureau Subject Leader (2015RAXXJ029).

References

[1] Z. Yian, W. Zhiying, S. L. Keey, and C. G. Boay, "Long-term viscoelastic response of E-glass/bismaleimide composite in seawater environment," *Applied Composite Materials*, vol. 22, no. 6, pp. 693–709, 2015.

[2] H. Yan, R. Ning, G. Liang, Y. Huang, and T. Lu, "The effect of silane coupling agent on the sliding wear behavior of nanometer ZrO_2/bismaleimide composites," *Journal of Materials Science*, vol. 42, no. 3, pp. 958–965, 2007.

[3] W. Li, F. Liu, L. Wei, and T. Zhao, "Synthesis, morphology and properties of polydimethylsiloxane-modified allylated novolac/4,4′-bismaleimidodiphenylmethane," *European Polymer Journal*, vol. 42, no. 3, pp. 580–592, 2006.

[4] L. Ji, A. Gu, G. Liang, and L. Yuan, "Novel modification of bismaleimide–triazine resin by reactive hyperbranched polysiloxane," *Journal of Materials Science*, vol. 45, no. 7, pp. 1859–1865, 2010.

[5] H. Yan, L. Pengbo, Z. Junping, and N. Rongchang, "Mechanical properties of novel bismaleimide nanocomposites with Si_3N_4 nanoparticles," *Journal of Reinforced Plastics and Composites*, vol. 29, no. 10, pp. 1515–1522, 2010.

[6] L. Wang, M. He, T. Gong et al., "Introducing multiple biofunctional groups on the poly(ether sulfone) membrane substrate to fabricate an effective antithrombotic bio-interface," *Biomaterials Science*, vol. 5, no. 12, pp. 2416–2426, 2017.

[7] Y. Yu, S. Wang, J. Shao, Y. Zhou, and C. Gao, "Effect of the drying temperature on sulfonated polyether sulfone nanofiltration membranes prepared by a coating method," *Journal of Coatings Technology and Research*, vol. 15, no. 2, pp. 425–435, 2018.

[8] A. Abdolmaleki, S. Mallakpour, and M. Rostami, "Performance evaluation of fructose-functionalized multiwalled carbon nanotubes/biodegradable poly(amide–imide) based on *N,N′*-(pyromellitoyl)-bis-*S*-valine bionanocomposite," *High Performance Polymers*, vol. 27, no. 8, pp. 903–910, 2015.

[9] Q. W. Li, Y. Li, X. F. Zhang et al., "Structure-dependent electrical properties of carbon nanotube fibers," *Advanced Materials*, vol. 19, no. 20, pp. 3358–3363, 2007.

[10] M. Alsawat, T. Altalhi, K. Gulati, A. Santos, and D. Losic, "Synthesis of carbon nanotube–nanotubular titania composites by catalyst-free CVD process: insights into the formation mechanism and photocatalytic properties," *ACS Applied Materials & Interfaces*, vol. 7, no. 51, pp. 28361–28368, 2015.

[11] C.-C. Hou, S. Cao, W.-F. Fu, and Y. Chen, "Ultrafine CoP nanoparticles supported on carbon nanotubes as highly active electrocatalyst for both oxygen and hydrogen evolution in basic media," *ACS Applied Materials & Interfaces*, vol. 7, no. 51, pp. 28412–28419, 2015.

[12] E. Ramya, N. Momen, and D. N. Rao, "Preparation of multiwall carbon nanotubes with zinc phthalocyanine hybrid materials and their nonlinear optical (NLO) properties," *Journal of Nanoscience and Nanotechnology*, vol. 18, no. 7, pp. 4764–4770, 2018.

[13] L. Zhanjun, C. Hui, W. Jing, X. Xiaohong, L. Hongbo, and Y. Li, "Surface modification of short carbon fibers with carbon nanotubes to reinforce epoxy matrix composites," *Journal of Nanoscience and Nanotechnology*, vol. 18, no. 7, pp. 4940–4952, 2018.

[14] Y. Chen, Z. Li, C. Teng, F. Li, and Y. Han, "Dielectric properties of polyether sulfone/bismaleimide resin composite based on nanolumina modified by super-critical ethanol," *Journal of Electronic Materials*, vol. 45, no. 11, pp. 6026–6032, 2016.

[15] P. Molla-Abbasi, K. Janghorban, and M. S. Asgari, "A novel heteropolyacid-doped carbon nanotubes/Nafion nanocomposite membrane for high performance proton-exchange methanol fuel cell applications," *Iranian Polymer Journal*, vol. 27, no. 2, pp. 77–86, 2018.

[16] S. Versavaud, G. Regnier, G. Gouadec, and M. Vincent, "Influence of injection molding on the electrical properties of polyamide 12 filled with multi-walled carbon nanotubes," *Polymer*, vol. 55, no. 26, pp. 6811–6818, 2014.

[17] P. Chen, Q. Shen, G. Luo, C. Wang, M. Li, and L. Zhang, "Role of interface tailoring by Cu coating carbon nanotubes to optimize Cu–W composites," *Journal of Materials Research*, vol. 30, no. 24, pp. 3757–3765, 2015.

[18] J. Pascual, F. Peris, T. Boronat, O. Fenollar, and R. Balart, "Study of the effects of multi-walled carbon nanotubes on mechanical performance and thermal stability of polypropylene," *Polymer Engineering and Science*, vol. 52, no. 4, pp. 733–740, 2012.

[19] P. Li, T. Li, and H. Yan, "Mechanical, tribological and heat resistant properties of fluorinated multi-walled carbon nanotube/bismaleimide/cyanate resin nanocomposites," *Journal of Materials Science & Technology*, vol. 33, no. 10, pp. 1182–1186, 2017.

[20] G. Wang, R. Wang, G. Fu et al., "Study on phenolphthalein poly(ether sulfone)-modified cyanate ester resin and epoxy resin blends," *Polymer Engineering and Science*, vol. 55, no. 11, pp. 2591–2602, 2015.

[21] Y. Huang, J. Ding, X. Chen, and X. Sun, "Synthesis, mechanical property, and thermal stability of reduced graphene oxide-zinc oxide/cyanate ester/bismaleimide resin composites," *Journal of Adhesion Science and Technology*, vol. 31, no. 12, pp. 1348–1360, 2017.

[22] W. Li, M. Wang, Y. Yue, W. Ji, and R. Ren, "Enhanced mechanical and thermal properties of bismaleimide composites with covalent functionalized graphene oxide," *RSC Advances*, vol. 6, no. 59, pp. 54410–54417, 2016.

[23] R. Konnola, C. P. R. Nair, and K. Joseph, "High strength toughened epoxy nanocomposite based on poly(ether sulfone)-grafted multi-walled carbon nanotube," *Polymers for Advanced Technologies*, vol. 27, no. 1, pp. 82–89, 2016.

[24] A. Reghunadhan, J. Datta, N. Kalarikkal, J. T. Haponiuk, and S. Thomas, "Toughness augmentation by fibrillation and

yielding in nanostructured blends with recycled polyurethane as a modifier," *Applied Surface Science*, vol. 442, pp. 403–411, 2018.

[25] J. Jose, K. Joseph, J:. Pionteck, and S. Thomas, "PVT behavior of thermoplastic poly(styrene-co-acrylonitrile)-modified epoxy systems: relating polymerization-induced viscoelastic phase separation with the cure shrinkage performance," *Journal of Physical Chemistry B*, vol. 112, no. 47, pp. 14793–14803, 2008.

[26] G. Q. Peng, F. H. Shi, Y. F. Wang et al., "Effects of three types of T700 carbon fiber on the mechanical properties of their composites with bismaleimide resin," *New Carbon Materials*, vol. 31, no. 2, pp. 176–181, 2016.

[27] B. Zhang, W. Gao, P. Chu, Z. Zhang, and G. Zhang, "Trap-modulated carrier transport tailors the dielectric properties of alumina/epoxy nanocomposites," *Journal of Materials Science-Materials in Electronics*, vol. 29, no. 3, pp. 1964–1974, 2018.

[28] Y. Wang, K. Kou, G. Wu, A. Feng, and L. Zhuo, "The effect of bis allyl benzoxazine on the thermal, mechanical and dielectric properties of bismaleimide–cyanate blend polymers," *RSC Advances*, vol. 5, no. 72, pp. 58821–58831, 2015.

[29] M. Jiang, X. Zou, Y. Huang, and X. Liu, "The effect of bismaleimide on thermal, mechanical, and dielectric properties of allyl-functional bisphthalonitrile/bismaleimide system," *High Performance Polymers*, vol. 29, no. 9, pp. 1016–1026, 2017.

[30] Z. Zhang, L. Yuan, G. Liang, and A. Gu, "Fabrication and origin of flame retarding glass fiber/bismaleimide resin composites with high thermal stability, good mechanical properties, and a low dielectric constant and loss for high frequency copper clad laminates," *RSC Advances*, vol. 6, no. 24, pp. 19638–19646, 2016.

[31] J. Qiu, Q. Wu, and L. Jin, "Effect of hyperbranched polyethyleneimine grafting functionalization of carbon nanotubes on mechanical, thermal stability and electrical properties of carbon nanotubes/bismaleimide composites," *RSC Advances*, vol. 6, no. 98, pp. 96245–96249, 2016.